PWM-VSI Inverter-Assisted Stand-Alone Dual Stator Winding Induction Generator

Olorunfemi Ojo, *Senior Member, IEEE,* and Innocent Ewean Davidson, *Member, IEEE*

***Abstract*—This paper presents a novel usage of a dual stator winding three-phase induction machine as a stand-alone generator with both controlled output load voltage magnitude and frequency. This generator, with both three-phase power and control windings housed in the stator structure, has the load connected to the power winding and a three-phase pulsewidth modulation (PWM) voltage-source inverter sourcing the control winding. The input to the PWM inverter is either a battery source or a charged dc capacitor. The operational characteristics of these generator schemes with either of the two inverter sources are investigated and shown to have desirable performance. How the load voltage magnitude depends on the various control and design parameters such as rotor speed, compensating capacitance, and load impedance is determined using a detailed mathematical model of the system.**

***Index Terms*—Battery, dual stator winding induction generator, load voltage control, voltage-source inverter.**

I. Introduction

A SELF-EXCITED three-phase induction generator is provided with reactive power by a three-phase capacitor bank connected across the stator terminals to ensure stable operation and maintain output voltage when the rotor is supplied by a mechanical power source. Self-excitation and, hence, the load voltage is maintained when the slip is negative. An application limitation of the capacitively compensated three-phase induction generator is the drastic change of the voltage regulation with load and rotor speed variations. Furthermore, when the active power demand of the load is higher than the input rotor mechanical power, the load voltage collapses. These performance constraints of capacitively compensated induction generators limit their widespread application, especially in situations where regulated load voltage and frequency are required.

Remedial measures such as the use of static reactive power generators and other power-electronics-based switching devices that present variable compensating capacitance or reactive power to the load for voltage support have been proposed [1]–[3]. Connecting a dc–ac inverter in series or parallel with the load provides variable reactive power, in the process of which both the load voltage magnitude and frequency are effectively regulated [4], [5]. Unfortunately, many of these remedial schemes inject harmonics into the load current and voltage waveforms.

To effectively regulate both the voltage magnitude and load frequency while minimizing/eliminating converter-induced harmonics in the load with a possibility of increasing the output power and optimizing system efficiency, dual stator winding induction generator schemes with a converter connected to the control winding, shown in Fig. 1, are proposed. Since the power and control windings are not physically connected but electromagnetically linked, the influence of the inverter-induced harmonics on the load waveforms is minimal.

The operation and feasibility of the proposed schemes are explored in this paper. Mathematical models, useful for steady-state calculations and computer simulations for the two schemes, are presented and employed to investigate the influence of design and control parameters on the generator characteristics. Calculation and computer simulation results confirm the usefulness of the models. The balance of the paper is devoted to the feedback control of the two proposed schemes—especially Fig. 1(b), which is generally unstable when operated in open-loop mode.

The paper is organized as follows. Section II gives a detailed description of the two generator schemes; the system models are set forth in Section III. System studies, including steady-state and dynamic performance of the battery-inverter and dc charged capacitor-inverter schemes, are presented in Section IV and Section V, respectively. Conclusions are drawn in Section VI.

II. Proposed Generator Systems

The dual stator winding synchronous machine was introduced at the beginning of this century as a means of increasing the power capability of large synchronous generators. In the recent past, it was used as a source of both regulated dc and ac output voltages. [6]–[8]. Dual stator winding reluctance machines have also been investigated for both drive and autonomous generator operations [9], [14]. The angular speed of the generated voltage is equal to the electrical rotor angular speed in the dual stator winding synchronous generator. In the dual stator winding reluctance generator, the sum of the angular electrical frequencies of the currents in the two stator windings equals the electrical angular frequency of the shaft (in the steady state)—rigidly tying the frequency of the generated voltage to the shaft speed. In applications with variable turbine (rotor) speeds, load frequency control is slightly complicated by dual synchronous and reluctance generators. Although it is realized that dual stator winding induction machines may be used as generators in view of the additional degree of

Paper IPCSD 00–037, presented at the 1999 Industry Applications Society Annual Meeting, Phoenix, AZ, October 3–7, and approved for publication in the IEEE TRANSACTIONS ON INDUSTRY APPLICATIONS by the Electric Machines Committee of the IEEE Industry Applications Society. Manuscript submitted for review October 15, 1999 and released for publication July 18, 2000.

O. Ojo is with the Department of Electrical and Computer Engineering, Tennessee Technological University, Cookeville, TN 38505 USA (e-mail: ojo@tntech.edu).

I. E. Davidson is with the Department of Electrical, Electronic and Computer Engineering, University of Pretoria, Pretoria, South Africa (e-mail: inno.davidson@eng.up.ac.za).

Publisher Item Identifier S 0093-9994(00)10427-X.

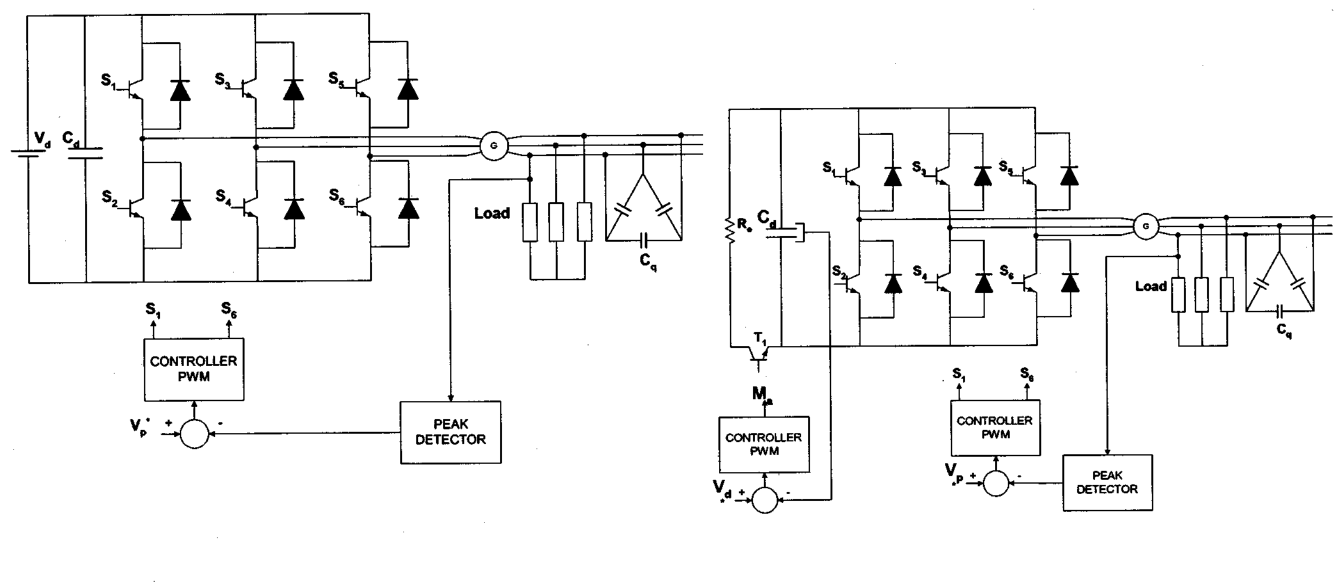

(a) (b)

Fig. 1. Schematic diagram of the dual stator winding induction generator with dc–ac inverter. (a) With a battery source. (b) With a charged dc capacitor.

freedom given by the uncoupled relationship between the rotor speed and frequency of generated voltage, it has not been fully explored until now.

Two types of dual stator winding induction machines with standard squirrel-cage rotor structure have been proposed. In the first design, there are two identical three-phase windings (control and power winding sets) which are wound for the same number of poles. However, these two windings are electrically displaced from each other [8]. In the most recently proposed design, the control and power windings are wound for different pole numbers with no displacement between the power and control windings using the regular squirrel-cage rotor structure—ideally decoupling the torque production of the two windings when individually excited [10]. Of course, there are the doubly fed induction machines with specially designed rotor cage structures [18], [19]. The generator scheme presented in this paper is based on the dual stator winding induction machine with displaced power and control winding sets. The power and control windings have the same number of poles. In Fig. 1(a), a three-phase pulsewidth modulation (PWM) dc–ac inverter under sine-triangle control and fed with a battery source is connected to the control windings. The dc–ac PWM inverter, augmenting the compensating three-phase delta-connected capacitors $C_{q,}$ provides reactive power to the generator system, fixes the load frequency, and influences the magnitude of the load voltage by regulating the modulation index magnitude. Indeed, the frequency of the reference signal of the PWM becomes the frequency of the generated load voltage. The battery source acts as a real power buffer. When the real power provided by the rotor shaft exceeds the load real power demand and system losses, the excess power is stored in the battery through the bidirectional inverter. If, on the other hand, the real power demand of the load and losses exceeds the input real power from the shaft, the balance is supplied by the battery. Another advantage of this scheme is the possibility of maintaining a load voltage magnitude with the desired load frequency, even when the rotor slip is positive for a relatively short period. While the machine motors, the battery provides the needed real power through the inverter to the load.

The scheme in Fig. 1(b) has a charged dc capacitor connected to the inverter input. If the load is light, the dc capacitor may overcharge and the system becomes unstable. If the load is heavy, the capacitor discharges, and the load voltage collapses. To ensure stable operation, a discharge resistor is connected across the charged capacitor through a transistor or MOSFET under PWM duty ratio control. The duty ratio control, which seeks to regulate the capacitor voltage, presents a variable resistance (which dissipates the excess real power) to the charged capacitor. The inverter PWM modulation index magnitude control regulates the load voltage. A feedback control scheme(to be discussed) is required to operate the system stably. Since there is no source of active power on the inverter side, if the rotor slip is positive, the load voltage decays and may ultimately collapse.

III. System Model

The q–d equations of the dual stator winding induction machine in the synchronous reference frame are set forth in [8] and [11]. Expressed in the complex variable form, the electrical equations are given as

$$V_{qdp} = r_p i_{qdp} + p\lambda_{qdp} - j\omega_e \lambda_{qdp} \tag{1}$$
$$V_{qds} = r_s i_{qds} + p\lambda_{qds} - j\omega_e \lambda_{qds} \tag{2}$$
$$V_{qdr} = r_r i_{qdr} + p\lambda_{qdr} - j(\omega_e - \omega_r)\lambda_{qdr} \tag{3}$$

where

$$\begin{aligned}\lambda_{qdp} &= L_p i_{qdp} + L_{ps} i_{qds} + L_m i_{qdr}\\ \lambda_{qds} &= L_s i_{qds} + L_{ps} i_{qdp} + L_m i_{qdr}\\ \lambda_{qdr} &= L_r i_{qdr} + L_m(i_{qdp} + i_{qds}).\end{aligned}$$

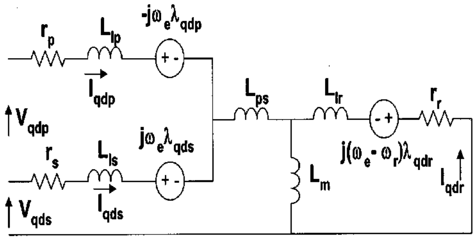

Fig. 2. The q–d equivalent circuit of the dual stator winding induction machine.

The q–d complex voltage inputs to the power and control windings are V_{qdp} and V_{qds}, respectively; λ_{qdp} and λ_{qds} are the q–d flux linkages of the power and control windings, respectively, while λ_{qdr} is the rotor q–d flux linkage. The power and control q–d stator currents are I_{qdp} and I_{qds}, respectively; and the rotor current is represented by I_{qdr}. The derivative d/dt is donated by p, and ω_e and ω_r are the angular electrical frequency of the load voltage and rotor speed, respectively. Fig. 2 gives the equivalent circuit of the dual stator winding induction generator in the synchronous reference frame, showing the machine parameters and state variables.

From Fig. 1, the q–d equations of the load and compensating capacitor C_q are

$$V_{qdp} = (R_o - j\omega_e L_o)i_{qdo} + L_o i_{qdo} \tag{4}$$

$$C_q p V_{qdp} = -(i_{qdo} + i_{qdp}) + j\omega_e C_q V_{qdp}. \tag{5}$$

The load resistance and inductance are R_o and L_o, respectively. The equations relating the input dc voltage and the output phase voltages of the dc–ac converter (the input phase voltages to the control winding) are

$$V_{as} = \frac{V_d}{3}(2S_a - S_b - S_c) \tag{6}$$

$$V_{bs} = \frac{V_d}{3}(2S_b - S_a - S_c) \tag{7}$$

$$V_{cs} = \frac{V_d}{3}(2S_c - S_a - S_b). \tag{8}$$

The switching functions of devices S_1, S_3, and S_5 are S_a, S_b, and S_c, respectively; I_{as}, I_{bs}, I_{cs} are the corresponding control winding phase currents. The input current flowing into the inverter is expressed as

$$I_d = I_{as}S_a + I_{bs}S_b + I_{cs}S_c. \tag{9}$$

Equations (6)–(9) transformed into the complex-plane synchronous reference frame become [13]

$$I_d = \mathrm{Re}\,al\,(M_{qds}{}^* i_{qds}) \tag{10}$$

$$V_{qds} = M_{qds}V_d. \tag{11}$$

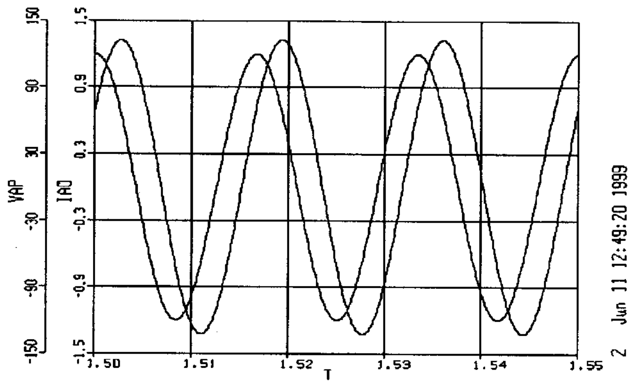

Fig. 3. Load voltage (V) and current (A) waveforms of the battery–inverter generator system. Load impedance $= 50\ \Omega$, modulation index magnitude $= 0.6$ time in seconds.

The modulation index magnitude of the inverter is M_{qds}. The dc capacitor voltage for the battery–inverter system is given by

$$C_d p V_d = -(I_o - I_d). \tag{12}$$

For the dc charged capacitor–inverter system, the dc capacitor voltage is expressed as

$$C_d p V_d = -\left(\frac{M_a V_d}{R_e} + I_d\right) \tag{13}$$

where

M_a switching function of transistor T_1;

R_e value of the discharge resistance;

I_o battery current flowing into the dc capacitor.

The full battery model used for computer simulations is set forth in [12].

IV. Battery–Inverter System

The generator scheme with the battery–inverter connected to the control windings has the added advantage of being able to regulate both the load voltage and frequency when the slip is positive and/or when the input shaft power is insufficient to meet system loss and load active power demand. Under these conditions, real power is supplied to the load by the battery. Alternatively, when the shaft power exceeds the load demand and the system losses, the extra power is fed to charge the battery. Hence, under light load condition, the inverter charges the battery and discharges it when the load demand is high or there is a decrease in the rotor speed. Fig. 3 shows simulated load voltage–load current waveforms of the system feeding an impedance load. It is evident that inverter-induced harmonics injected in the load waveforms are minimal.

Under steady-state condition, the state derivatives of the system equations (1)–(12) are identically equal to zero. From the resulting steady-state equations, the generator voltage gain is given by

$$G = \frac{V_{qdp}}{V_{qds}} = A\left[\frac{Z_r Z_{ps} + Z_m Z_{mr}}{Z_\Delta}\right] \tag{14}$$

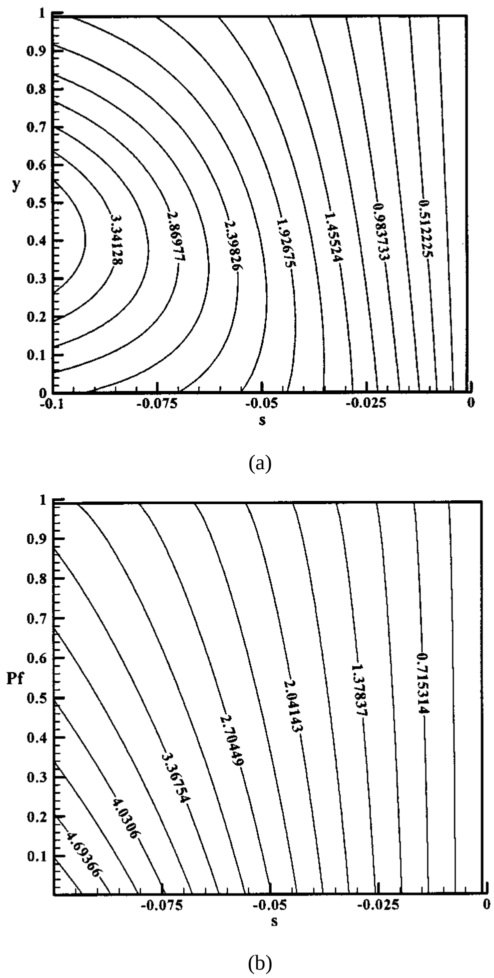

Fig. 4. Variation of the voltage gain magnitude. (a) With changing slip (s) and C_q (**y** 50 μF), constant impedance $= 100\ \Omega$. (b) With changing slip (s), constant load impedance, constant C_q, and changing load power factor (*Pf*).

where

$$
\begin{aligned}
A &= \frac{Z_r}{Z_s Z_r + Z_m Z_{mr}} \\
B &= \frac{Z_m Z_{mr} + Z_r Z_{ps}}{Z_s Z_r + Z_m Z_{mr}} \\
Z_\Delta &= Z_r - Z_c(Z_p Z_r + Z_{mr} Z_m + B Z_{mr} Z_{ps} + B Z_m Z_{mr}) \\
Z_c &= \frac{1}{Z_o} - j\omega_e C_q \\
Z_p &= rp - j\omega_e L_p \\
Z_s &= r_s - j\omega_e L_s \\
Z_m &= j\omega_e L_m \\
Z_r &= r_r - j(\omega_e - \omega_r) L_r \\
Z_{ps} &= j\omega_e L_{ps} \\
Z_{mr} &= j(\omega_e - \omega_r) L_m \\
Z_o &= R_o - j\omega_e L_o.
\end{aligned}
$$

Fig. 4 gives the plots showing the dependence of the voltage gain magnitude on the value of C_q, rotor slip, and load power factor for a laboratory dual stator winding generator with parameters given in the Appendix. The voltage gain magnitude increases with increasing slip and reducing capacitance value for a constant load impedance in Fig. 4(a). Higher voltage gain requires higher rotor speed with the value of C_q selected within a range. Low slip magnitudes generally result in lower voltage gains for most values of C_q. Since higher rotor slip results in higher losses, the generator is less efficient, especially when a higher than unity voltage gain is desired. For a constant load impedance and constant C_q, the voltage seems to decrease with increasing load power factor and decreasing rotor slip magnitude [Fig. 4(b)]. It is concluded from these plots that, to meet required load voltage, C_q, rotor slip, and inverter modulation index magnitude (or battery voltage) are design and control variables that must be appropriately selected. With these many control and design variables, it is feasible to achieve regulated load voltage and frequency while optimizing overall system efficiency.

The battery–inverter dual stator winding generator is always stable as long as the battery can meet the active load power demand while augmenting the mechanical shaft input. However, to regulate the load voltage, a simple dynamic controller such as the proportional–integral (PI) or integral–proportional (IP)

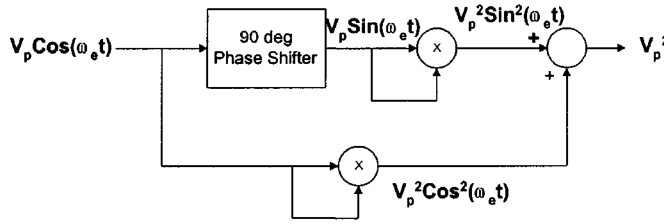

Fig. 5. Block diagram of peak load voltage detector.

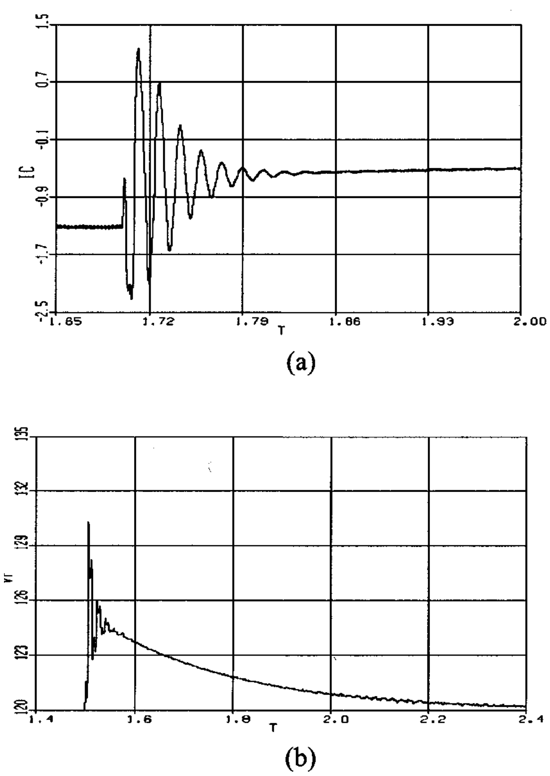

Fig. 6. Dynamics due to load impedance change from 500 to 50 Ω. Reference peak voltage $= 120$ V, time in seconds. (a) battery current (A). (b) Peak phase voltage (V).

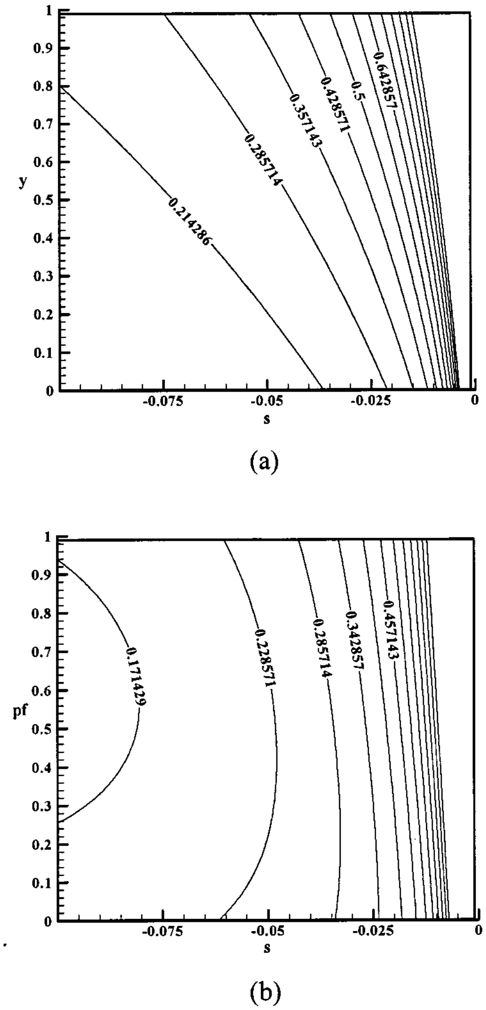

Fig. 7. Variation of the transistor duty ratio and modulation magnitude with C_q ($\mathbf{y}$ 50 μF) and slip (s). Load impedance $= 100\ \Omega$. (a) Duty ratio. (b) Modulation index magnitude.

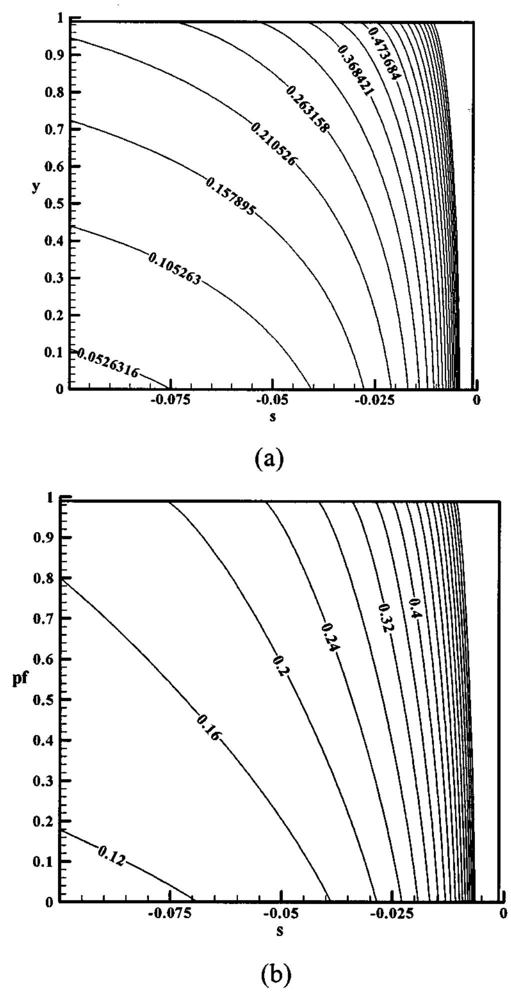

Fig. 8. Variation of the transistor duty ratio and modulation magnitude load power factor (*pf*) and slip (*s*). Load impedance $= 100\ \Omega$. (a) Duty ratio. (b) Modulation index magnitude.

can be implemented. The selection of controller gains that ensure good regulation and robustness to changing load and rotor speed is based on the loop-shaping technique set forth in [17]. The peak value of the load phase voltage is compared with the desired peak load voltage; the error is fed to a dynamic PI controller, the output of which becomes the value of modulation index magnitude which is also the peak of the three-phase sinusoidal reference signal for the PWM inverter. Comparison of these three reference signals with a triangle waveform produces the switching pulses to the inverter switching devices (MOSFETs) [15]. Fig. 1(a) also shows the sketch of the controller structure. The peak load voltage is obtained using a fast peak detector in which the sensed phase voltage is phase shifted and processed. If the phase voltage is a cosinusoidal signal, the phase shifted signal is sinusoidal. The sum of squares of the phase voltage and the shifted signal provides the square of the peak voltage using multipliers and an adder, as illustrated in Fig. 5 [16]. Fig. 6 gives the response of the regulated generator system to a change of load impedance. It is observed that a simple PI controller quickly restores the load voltage to the reference value. With a change of load resistance from a high to a low value, less real power manifested in battery current is fed back through the bidirectional inverter into the battery, shown in Fig. 6(a). Similar good responses are obtained with other perturbations in rotor speed.

V. DC Capacitor–Inverter System

The dc-inverter system of the generator schematically shown in Fig. 1(b) provides reactive power to the load and, in the process, supports the load voltage. This system is always unstable under open-loop operation. With no storage facility, when the load demand and losses are lower than the input shaft power, the dc capacitor voltage continues to increase; however; if the load demand and losses exceed the input shaft power, the dc capacitor steadily decays. Two control loops are required to maintain the dc capacitor voltage at a set value and to regulate the load voltage, as shown in Fig. 1(b). The control scheme for the load voltage is the same as that of the battery–inverter system described above. For the regulation of the dc capacitor voltage, the reference capacitor value is compared with the measured value; the error voltage passed through a PI controller becomes the modulating signal of the PWM control.

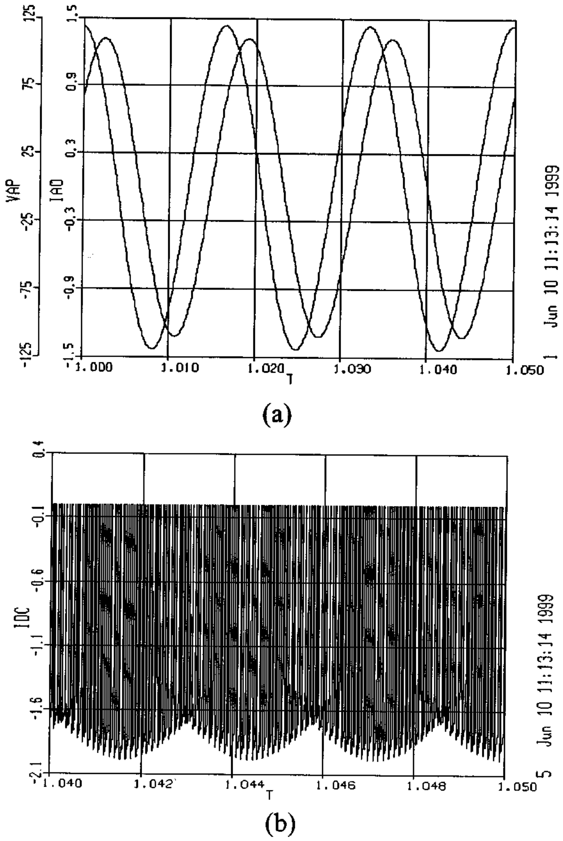

Fig. 9. Generator waveforms. (a) Load voltage (V) and current (A). Time in seconds requiring the decrease of the duty ratio (increasing the effective discharge resistance value) so as to maintain the reference capacitor voltage.

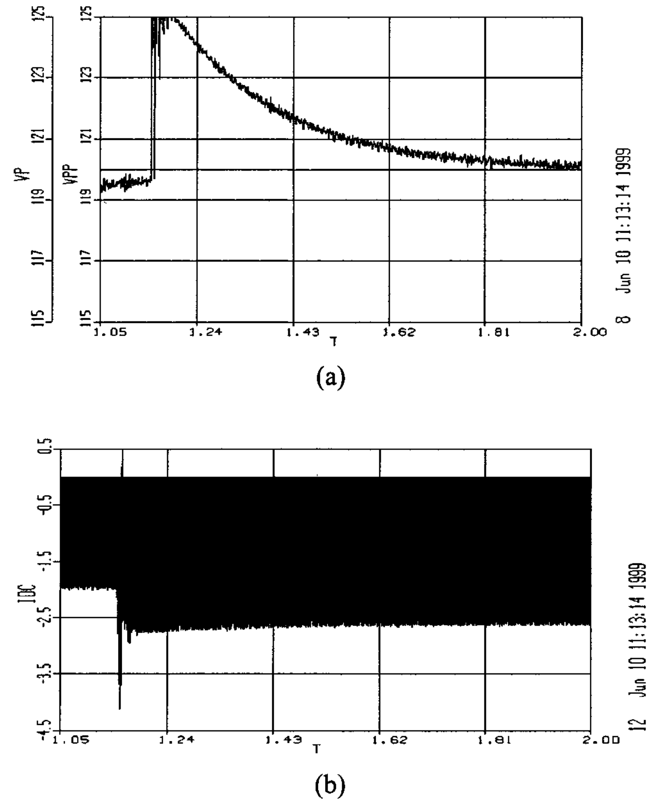

Fig. 10. Dynamics of generator to change in load impedance from 20 to 200 Ω. Voltage reference $=$ 120 V. (a) Reference and peak load voltage (V). (b) Inverter input current (A). Time in seconds.

This signal, when compared with the sawtooth waveform, changes the duty ratio of transistor T, which effectively makes the discharge resistance variable.

Under steady-state controlled situation, the dynamic model equations (1)–(11) and (14) reduce to

$$M_{qds} = \frac{V_p^*}{V_d^* \, |G|} \tag{15}$$

$$\frac{M_a}{R_e} + M_{qds}^2 \mathrm{Re}\, al(C) = 0 \tag{16}$$

where

$$C = \frac{A}{Z_\Delta}\left[Z_\Delta + BZ_c\left(Z_r Z_{ps} + Z_m Z_{mr}\right)\right].$$

The reference dc capacitor voltage is V_d^* and the reference phase voltage is V_p^*.

Fig. 7 consists of plots showing the duty ratio of transistor T, (M_a) and modulation index magnitude (M_{qds}) of the PWM inverter for a given reference capacitor and load voltages, constant impedance load and power factor, but changing C_q and slip. In Fig. 8, the load power factor and slip are varied with the load impedance, reference capacitor and load voltages being the same as in Fig. 7. It is evident from these graphs that the most efficient operating conditions occur at high values of M_a and M_{qds}, corresponding to lower magnitude of rotor slip.

Fig. 9 gives generator waveforms during steady-state operating condition. The waveforms are relatively clean when the dc capacitor voltage is kept constant at reference value by the changing duty ratio of transistor T. During dynamic change of load impedance plotted in Fig. 10, the controllers regulate the capacitor dc voltage and load voltage magnitude to set values and ensure system stability. The current flowing into the capacitor from the inverter increases, requiring the decrease of the duty ratio (increasing the effective discharge resistance value) so as to maintain the reference capacitor voltage.

VI. Conclusions

The feasibility of the dual stator winding induction generator producing regulated load voltage and frequency using either a battery–inverter or a dc charged capacitor–inverter connected to the three-phase control windings has been demonstrated. The battery–inverter system has the capability to operate effectively, even when, for a short while, the rotor slip becomes positive because of the battery power that can be fed to the load. In the charged dc capacitor–inverter system, two closed-loop controllers are required to ensure system stability and regulate the load. It is open-loop unstable. For the two schemes, the rotor speed, compensating capacitance value, and the inverter and/or discharge resistor controls can be manipulated to meet load requirement while ensuring optimum efficiency operation. Steady-state curves showing how the voltage gain magnitude depends on the various design and control parameters are also presented as steady-state and dynamic waveforms that demonstrate the quality of the load voltage and current waveforms. The effectiveness of simple control loops regulating the load voltage and dc capacitor voltage are shown for various dynamic operational changes.

The delta-connected capacitor bank at the terminals of the load reduces the reactive requirement and, hence, the kVA of the inverter. It is not required to eliminate inverter-induced harmonics in the load since they are effectively taken care of by the secondary windings of the generator. The sizing of the inverter and the design of the secondary winding must take into consideration the generator operating speed range, the corresponding reactive power to be supplied by inverter to ensure voltage regulation, and the active power to be passed through the windings to or from the inverter. Since the motoring mode of operation should necessarily be a short-time phenomena, appropriate sizing of the buffer battery will suffice for the anticipated ride-through operation. It is not efficient to operate the generator when the speed falls below the synchronous speed for a significant length of time—since the load power must be supplied from the battery, processed by the inverter, electromagnetically converted with the generator losses supplied by the battery.

Instead, the battery–inverter through a changeover switch mechanism isolates the generator and connects the inverter directly to the load. The design of the generator scheme and selection of the inverter which is outside the scope of this paper is highly application dependent. The influence of the winding design on the parameters of the generator and most especially how the pitching of the stator windings affects the mutual leakage inductance between them are derived using the winding function methodology in [8].

The relative cost of this generation scheme will also depend on applications. It is safe to conclude that the topologies herein suggested must be considered as technologically viable induction generation option which may be studied under prevailing application requirements and constraints.

The proposed generator schemes should find utility in stand-alone and grid-connected power systems. With the known advantages of induction machines, ease of control, simplicity of the converter topology, and feasibility of optimum efficiency operation while regulating both load voltage and frequency, the two proposed topologies should find wide acceptability. High- or low-load phase voltage (equivalently, the voltage gain) is achievable by appropriate selection of the design and control parameters.

Finally, analysis technique for the simulation and steady-state calculation for controlled converter-based dual stator winding generator have been presented and should find utility in the analysis of other converter-controlled generator systems.

APPENDIX

The parameters of the 2-hp four-pole three-phase induction machine (parallel-connected stator winding split into two as power and control windings) are given as follows (it is observed that the mutual leakage inductance of this modified generator is not representative of actual dual stator winding induction machines [4], [8], [11], [20]):

power winding stator per-phase resistance, $r_p = 1.55\ \Omega$;
power winding per-phase leakage inductance, $L_{lp} = 0.008$ H;
control winding stator per-phase resistance, $r_s = 1.55\ \Omega$;
control winding per-phase leakage inductance, $L_{ls} = 0.008$ H;
mutual leakage inductance between power and control winding, $L_{ps} = 0.0001$ H;
magnetizing inductance, $L_m = 0.10$ H;
rotor per-phase resistance, $r_r = 0.58\ \Omega$;
rotor per-phase leakage inductance, $L_{lr} = 0.0085$ H.

REFERENCES

[1] J. M. Elders, J. T. Boys, and J. L. Woodward, “Self excited induction machine as a small low-cost generator,” *Proc. Inst. Elect. Eng.*, pt. C, vol. 131, no. 2, pp. 33–41, Mar. 1984.
[2] B. Brennen and A. Abbondanti, “Static exciters for induction generators,” *IEEE Trans. Ind. Applicat.*, vol. IA-13, pp. 422–428, Sept./Oct. 1977.
[3] R. Bonert and S. Rajakaruna, “Self-excited induction generator with excellent voltage and frequency control,” *Proc. Inst. Elect. Eng.*, pt. C, vol. 145, no. 1, pp. 33–39, Jan. 1998.
[4] E. Muljadi and T. A. Lipo, “Series compensated PWM inverter with battery supply applied to an isolated induction generator,” *IEEE Trans. Ind. Applicat.*, vol. 30, pp. 1073–1082, July/Aug. 1994.
[5] C. Jacobina, E. Silva, A. Lima, and R. Ribeiro, “Induction generator static systems with a reduced number of components,” in *Conf. Rec. 31st IEEE-IAS Annu. Meeting*, Oct. 1996, pp. 432–439.
[6] P. L. Alger, E. H. Freiburghouse, and D. D. Chase, “Double windings for turbine alternators,” *AIEE Trans.*, vol. 49, pp. 226–244, Jan. 1930.
[7] E. F. Fuchs and L. T. Rosenberg, “Analysis of an alternator with two displaced stator windings,” *IEEE Trans. Power App. Syst.*, vol. PAS-93, pp. 1776–1786, Nov./Dec. 1974.
[8] R. Schiferl, “Detailed analysis of a six-phase synchronous machine with AC and DC stator connections,” M.S. thesis, Purdue Univ., West Lafayette, IN, 1982.
[9] Z. Wu, “Modeling, simulation and application of a doubly-fed reluctance electrical machine,” Ph.D. dissertation, Tennessee Technol. Univ., Cookeville, Dec. 1998.
[10] A. Munoz-Garcia and T. A. Lipo, “Stator winding induction machine drive,” in *Conf. Rec. IEEE-IAS Annu. Meeting*, Oct. 1998, pp. 601–608.
[11] T. A. Lipo, “A q–d model for six phase induction machines,” in *Proc. Int. Conf. Electric Machines*, Athens, Greece, 1980, pp. 860–867.
[12] O. Ojo, O. Obasohan, and A. Jimoh, “Expanding the operating range of a single-phase induction generator with a PWM inverter,” in *Conf. Rec. IEEE-IAS Annu. Meeting*, Oct. 1998, pp. 205–212.
[13] P. Vas, *Electrical Machines and Drives, A Space—Vector Theory Approach*. Oxford, U.K.: Oxford Univ. Press, 1992.
[14] L. Xu and Y. Tang, “A novel wind-power generating system using field orientation controlled doubly-excited brushless reluctance machine,” in *Conf. Rec. IEEE-IAS Annu. Meeting*, 1992, pp. 408–413.
[15] N. Mohan, T. M. Undeland, and W. P. Robbins, *Power Electronics, Converters, Applications and Design*. New York: Wiley, 1995.
[16] B. Kwon, J. Youm, and J. Choi, “Automatic voltage regulator with fast dynamic speed,” *Proc. IEE—Elect. Power Applicat.*, vol. 146, no. 2, pp. 201–207, Mar. 1999.
[17] S. Skogestad and I. Postlethwaite, *Multivariable Feedback Control, Analysis and Design*. New York: Wiley, 1997.
[18] L. J. Hunt, “A new type of induction motor,” *J. IEE*, vol. 38, pp. 648–677, 1907.
[19] S. Williamson, A. C. Ferreira, and A. K. Wallace, “Generalized theory of the brushless doubly-fed machine—Part 1: Analysis,” *Proc. IEE—Elect. Power Applicat.*, vol. 144, no. 2, pp. 111–121, Mar. 1997.
[20] K. Gopakumar, V. T. Ranganathan, and S. R. Bhat, “Vector control of induction motor with split phase stator windings,” in *Conf. Rec. IEEE-IAS Annu. Meeting*, 1994, pp. 569–574.

Olorunfemi Ojo (M'87–SM'95) was born in Kabba, Nigeria. He received the B.Eng. and M.Eng. degrees in electrical engineering from the Ahmadu Bello University, Zaria, Nigeria, and the Ph.D. degree from the University of Wisconsin, Madison, in 1977, 1980, and 1987.

From 1978 to 1982, he was a Lecturer at Ahmadu Bello University. He was a Post-Doctoral Fellow at the University of Wisconsin, Madison, between 1987–1988. Since 1988, he has been with the Department of Electrical and Computer Engineering, Tennessee Technological University, Cookeville, where he is currently a Professor. His current research interests span the areas of energy conversion, motor drives and control, and power electronics applications to power systems.

Dr. Ojo has been very active within the IEEE Industry Applications Society (IAS) as a Session Organizer and a Session Chairman for the Industrial Drives and Electric Machines Committee. He was a Recipient of a Prize Paper Award from the Electric Machines Committee of the IAS. He is also involved with the IEEE Power Engineering Society (PES) and is an Associate Editor of the IEEE TRANSACTIONS ON POWER ELECTRONICS.

Innocent Ewean Davidson (M'93) was born in Benin-City, Nigeria, in 1963. He received the B.Eng. (Hons.) and M.Eng. degrees from the University of Ilorin, Ilorin, Nigeria, and the Ph.D. degree from the University of Cape Town, Cape Town, South Africa, in 1984, 1987, and 1998, respectively, all in electrical engineering.

He is currently a Senior Lecturer in the Department of Electrical, Electronic and Computer Engineering, University of Pretoria, Pretoria, South Africa. His research interests are electric machine design, electromagnetic analysis, electric machines, electric drives, distributed power system dynamics, and economics.

Dr. Davidson is a member of the Nigerian Society of Engineers, South African Institute of Electrical Engineers, and an associate member of the Institution of Electrical Engineers, U.K.